CRUCIFORM SPECIMEN DESIGN FOR BIAXIAL ANALYSIS OF COMPOSITE MATERIAL

A. Rashedi[1*], I. Sridhar[1], K. J. Tseng[2]

[1]*School of Mechanical and Aerospace Engineering, Nanyang Technological University, 50 Nanyang Avenue, Singapore 639798, Singapore.*
[2]*School of Electrical and Electronic Engineering, Nanyang Technological University, 50 Nanyang Avenue, Singapore 639798, Singapore.*
**amma0002@ntu.edu.sg*

Keywords: composite, biaxial testing, crack analysis, cruciform specimen

Abstract
This article highlights key results of finite element (FE) simulations to develop an optimized cruciform specimen for composite material biaxial characterization. 10 different biaxial specimen geometries with centre cracks have been studied; out of which 4 representative ones are presented. The objective was to attain the uniform far-field stress for all geometries with different loading conditions. Key variables included different crack length, crack orientation, and change in composite lay-up sequence. The work detailed herewith has been undertaken in support of developing a biaxial test frame for studying the biaxial response of planar cruciform shape fibre-reinforced plastic laminates.

1 Introduction
Usage of composite materials have expanded vastly in our time, extending from tiny items to military equipments, large-scale aircrafts to space vehicles and even massive wind turbine blades are now manufactured with advanced composites. Likewise metals, these composite materials are regularly subjected to complex loadings under multi-axial stress and strain fields. Purely uniaxial loading, typically observed in conventional laboratory tests, rarely reflect such realistic loading conditions. This is compounded by the fact that fiber reinforced composite materials owing to their tailored laminate design and anisotropic nature usually behave less predictably comparing to metal genres. This endures as a major drawback for extensive usage of composite materials in many industries, thus leading to increased design conservatism, decreased reliability and heavier structure. Additionally, a comprehensive composite material failure study has been performed recently where nineteen leading composite failure theories are compared based on fourteen test cases and existing experimental data of tubular specimens [1-2]. Basic conclusions regarding the work appear as a few failure criteria maintaining the ability to well-predict the behavior of composite materials under different load condition, and that, there is a lack of reliable experimental data that could be compared with these theories. In view of this, development of reliable and rigorous composite test methods associated with robust multi-axial failure mechanisms and stable test standards is of utmost importance.

The article highlights a biaxial test setup development progress in line with initial biaxial specimen optimization works. The planned bi-axial test frame will consist of a primary (vertical) axis load carrying capacity up to 250 kN with two secondary (horizontal) axis actuators supporting up to 10 kN. The specimen design is a key step in this process that has to ensure an optimized specimen depending on the load-frame geometry and loading constraints.

2 Cruciform specimen design and discussion

In case of composite specimens with crack a successful cruciform geometry should ensure a uniform far field stress around the test area of interest prompting the failure to occur in biaxially loaded zone. Accordingly far-field stress variation has been measured for all geometries based on plane stress element rings at a certain distance apart from the crack in finite element (FE) platform. The FE simulations have been conducted with commercial software *Abaqus* using shell element type *S8R5*. It is an 8-node doubly curved thin shell, reduced integration element having five degrees of freedom per node. The material modelled was glass fibre reinforced epoxy with 24 layer symmetric cross-ply and quasi-isotropic layout. Several cracked specimens are simulated by varying the key parameters, viz., specimen geometry (radius of curvature, corner fillet), crack length and crack orientation. Constant thickness was maintained for all geometries. Due to symmetry of the geometry, only half model of each geometry has been evaluated (Fig. 1). In subsequent sections, these geometries will sequentially be referred as 1(a), 1 (b), 1(c) and 1(d). Boundary condition was applied in the bottom part of the geometries to fix all rotational and translational movements so that it matches with the experimental test frame. Displacement control loading equivalent to ultimate failure stain of cross-ply and quasi-isotropic glass fibre reinforced epoxy laminate (~0.38%) was applied in all cases [3].

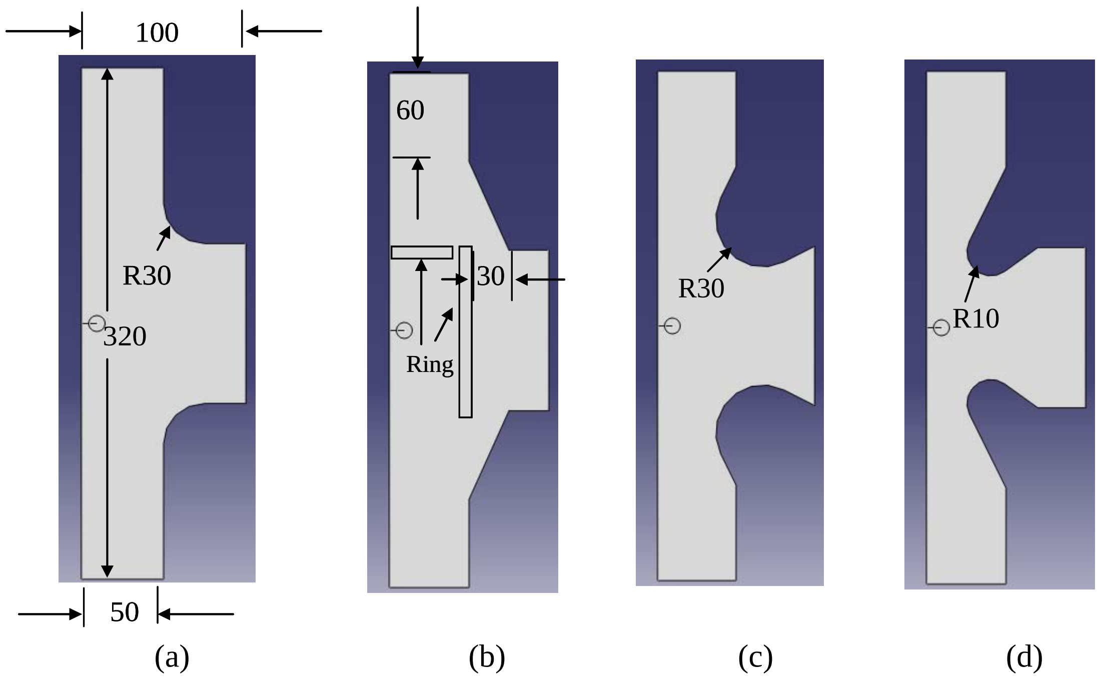

Figure 1. Half model of four representative symmetric cruciform specimen geometries with 10 mm centre crack (dimensions are in mm)

A data reduction system is applied, consequently, as follows: i) first all nine geometries are analyzed with a 10 mm and 25 mm crack oriented at 0° and 45° with respect to x axis, ii) the geometries with more uniform stresses have been sorted out with a standard deviation cut-off limit at 5%, iii) the best geometries, thus far obtained, have been simulated with different other laminates of 10 mm and 25 mm crack oriented at 0° and 45° with respect to horizontal axis. Here in this article we only present the simulation results of four representative geometries.

At the outset, displacement control loading was applied on a symmetric cross-ply laminate with centre crack length of 10 mm oriented at 0° with respect to the horizontal axis. Mean value and standard deviation (SD) of normal stresses in the horizontal axis direction are determined for all four geometries at 50 mm distance from the axis of symmetry. A vertical ring of elements has been chosen for this pursuit which is highlighted in Fig. 1 (b). The same ring of elements has been used for all four geometries. Corresponding mean and standard deviation plots have been highlighted in first 8 columns of Fig. 2 with each mean and standard deviation standing side by side for all geometries. The FE simulation has been repeated consequently for 25 mm crack oriented at 0° with respect to horizontal axis. The next 8 columns of Fig. 2, sequentially, represent the mean and corresponding SD of the four geometries based on these simulation runs.

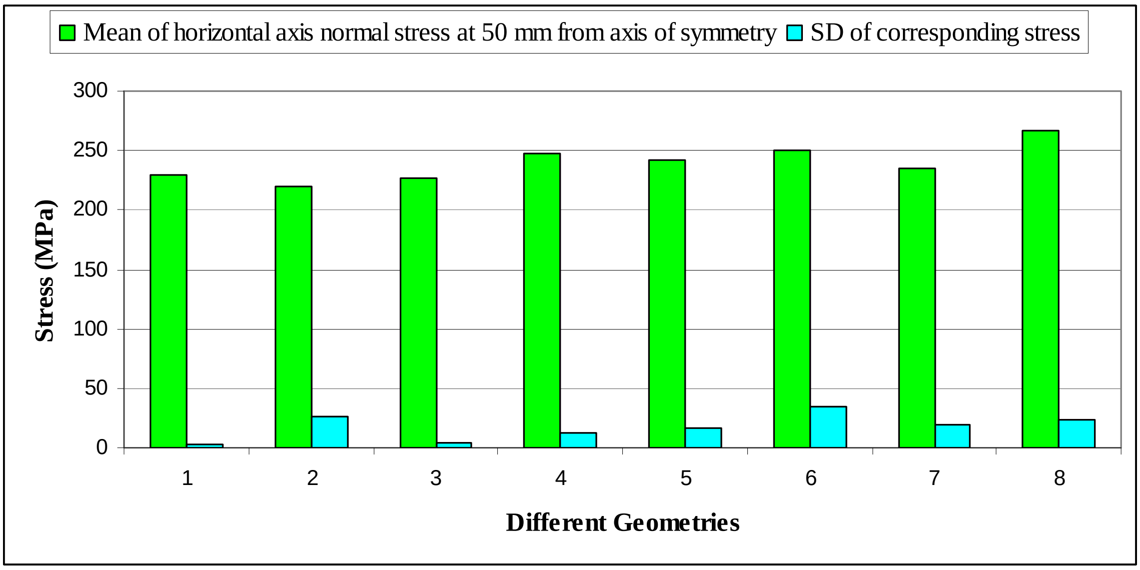

1: Geometry 1(a) with 10 mm, 0 degree crack; 2: Geometry 1(b) with 10 mm, 0 degree crack

3: Geometry 1(c) with 10 mm, 0 degree crack; 4: Geometry 1(d) with 10 mm, 0 degree crack

5: Geometry 1(a) with 25 mm, 0 degree crack; 6: Geometry 1(b) with 25 mm, 0 degree crack

7: Geometry 1(c) with 25 mm, 0 degree crack; 8: Geometry 1(d) with 25 mm, 0 degree crack

Figure 2. Mean and standard deviation of horizontal direction normal stress for 0° crack

It appears from Fig. 2 that Geometry 1(b) has the highest SD value for both of the crack dimensions; thus other geometries ensure more stress uniformity. Specially, Geometry 1(a) maintains excellent horizontal normal stress uniformity in comparison to other geometries with a SD value around 1.5% of the mean stress for both crack sizes. Henceforward, we analyze 45° crack with the same loading condition for the same laminate. The same ring of elements has been selected and corresponding mean, SD values have been calculated. The respective values have been plotted in Fig. 3 with first 8 columns for 10 mm crack and next 8 columns for 25 mm crack**.** It appears again from Fig. 3 that Geometry 1(a) has better stress uniformity than other geometries with Geometry 1(b) reflecting moderately high SD values. However, the SD values for 45° cracks are a bit higher than their 0° counterparts for all simulation runs which is expected for an angle crack. It is also noteworthy for Geometry 1(b) that some loads are bypassing the central section towards the perpendicular arm which contributes to its higher stress variation.

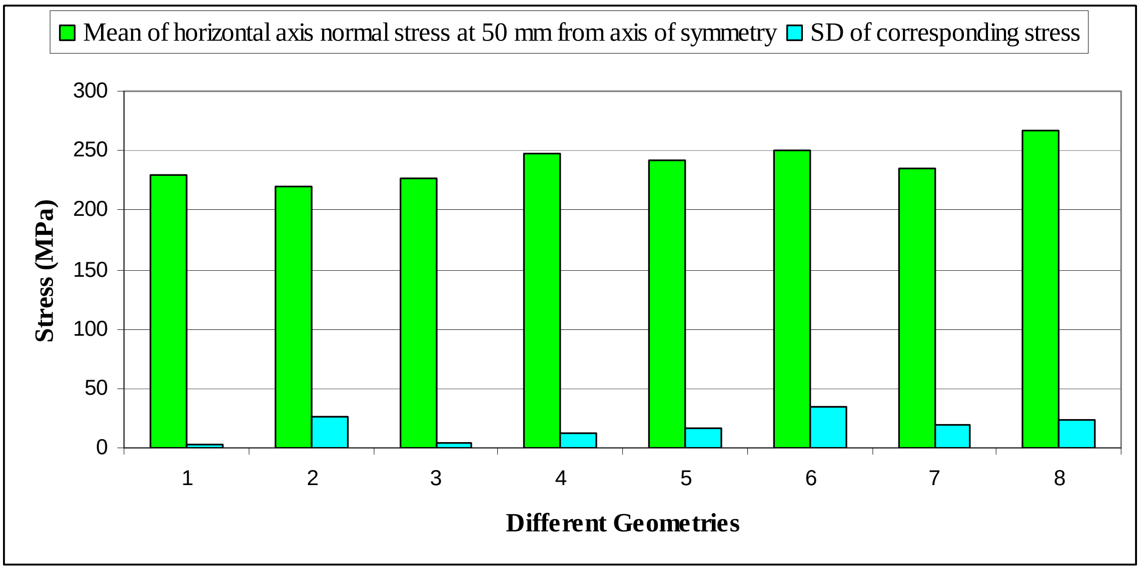

1: Geometry 1(a) with 10 mm, 45 degree crack; 2: Geometry 1(b) with 10 mm, 45 degree crack
3: Geometry 1(c) with 10 mm, 45 degree crack; 4: Geometry 1(d) with 10 mm, 45 degree crack
5: Geometry 1(a) with 25 mm, 45 degree crack; 6: Geometry 1(b) with 25 mm, 45 degree crack
7: Geometry 1(c) with 25 mm, 45 degree crack; 8: Geometry 1(d) with 25 mm, 45 degree crack

Figure 3. Mean and standard deviation of horizontal direction normal stress for 45° crack

Based on the simulation runs, Geometry 1(a) is found to have better stress uniformity. Also from vertical axis normal stress mean values and their corresponding SDs, the same conclusion can be drawn. Here we present mean and SD values only for the larger crack (25 mm), both for cross-ply and quasi-isotropic laminate, with 0° and 45° orientations.

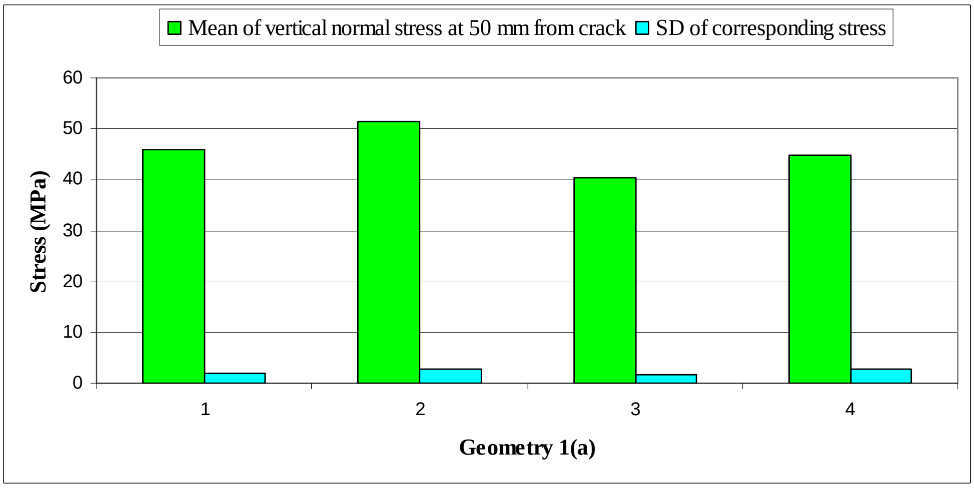

1: cross-ply with 0 degree 25 mm crack; 2: cross-ply with 45 degree 25 mm crack
3: quasi-isotropic with 0 degree 25 mm crack; 4: quasi-isotropic with 45 degree 25 mm crack

Figure 4. Mean and standard deviation of vertical direction normal stress for Geometry 1(a)

As appears from Fig. 4, for all combinations of laminates with different orientation of crack angles and Geometry 1(a) configuration, far-field stress values show good uniformity in the horizontal ring of elements (as depicted in Fig. 1(b)). However, 45° cracks are found to result in higher SD percentages - almost 3%, which is twice of the same for 0° cracks. Based on the simulation runs, Geometry 1(a) appears to be the best cruciform geometry depending on dimensional and loading constraints of the proposed experimental test frame.

3 Conclusions

The article has highlighted the key steps to develop a planar cruciform specimen geometry for biaxial characterization of fibre reinforced composite material. Final geometry has been achieved with a corner rounding of 30 mm at the intersection of two perpendicular arms with throughout constant thickness shape. The FE simulation works consequently need to be validated by experiments with full-field strain-measurement techniques.

Acknowledgements

A. Rashedi thanks Energy Research Institute at Nanyang (ERI@N), Nanyang Technological University (NTU) for the financial support of the project. Authors thank Mr. Simon Seah Kah Woon for many fruitful discussions.

References

[1] Hinton M.J., Kaddour A.S., Soden P.D. Prediction of world-wide failure theories: Part B: Some experimental comparisons in IMechE, London, UK, (1999).
[2] Hinton M.J., Soden P.D., Kaddour A.S. On the maturity of world-wide failure theories: Comparison with experiments for ±55° GRP laminates in ICCM-12, Paris, France, (1999).
[3] Kaw A. Mechanics of Composite Materials. Taylor and Francis, Boca Raton (2006).